Phenylacetylene Macrocycles with Two Opposing Bipyridine Donor Sites: Syntheses, X-ray Structure Determinations, and Ru Complexation

Oliver Henze, Dieter Lentz,* Andreas Schäfer, P. Franke, and A. Dieter Schlüter*[a]

Abstract: Reaction of the known macrocycle **1a**, which contains two bipyridine units in opposing sides, with two equivalents of $[Ru(bipy)_2Cl_2]$ furnishes the doubly *exo*-cyclically complexed macrocycle **8a** in 55% yield. Synthesis of the shape-persistent macrocycle **1c** by Hagihara–Sonogashira cross-coupling chemistry of suitably functionalized building blocks is reported. This macrocycle was also converted into a Ru complex (**8c**). X-ray analysis of single crystals of **1b** and **1c** shows a layered structure that contains "channels" filled with solvent molecules and parts of the flexible chains, with which the cycle is decorated for solubility reasons.

Keywords: bipyridines · cross-coupling reactions · N ligands · ruthenium · shape persistence · supramolecular chemistry

Introduction

We have recently used our construction set of oligo(het)arylene building blocks for the modular synthesis of the shape-persistent, hexagonal macrocycles **1a** and **1b** with two bipyridine (bipy) units in opposing sides.[1, 2] Interesting

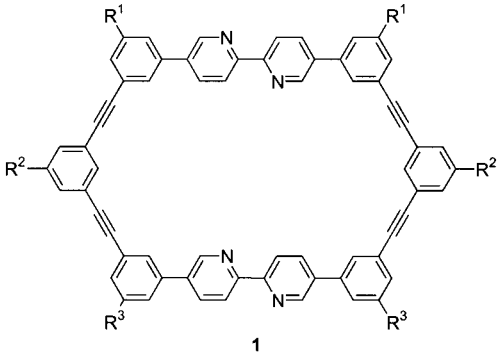

1

1a $R^1 = R^3 = CH_2OHex$, $R^2 = H$
1b $R^1 = R^3 = CH_2OMOM$, $R^2 = CH_2OHex$
1c $R^1 = R^3 = CH_2OTHP$, $R^2 = CH_2OHex$

research targets with these shape-persistent macrocycles include 1) equipping them with sites for *exo*- and *endo*-cyclic complexation with metal ions,[3] 2) investigation of their redox behavior both in the complexed and uncomplexed state, 3) their decoration with polar and nonpolar substitutents[4] which may go so far as to render them water soluble, and 4) investigation of their aggregation behavior and to try to accomplish columnar stacking.[5–12] Columnar stacks of properly equipped cycles may be used as nanopores for incorporation into membranes or for the generation of nanowires[13] through *endo*-cyclic metal-ion complexation followed by the reduction of the ion to the metallic state. Individual cycles may be used to generate one-, two-, or three-dimensional structures through *exo*-cyclic metal complexation.

Within this general theme, we now report several synthetic and structure analytical facets which, together with the previously published results,[1] provide a more comprehensive picture of the molecular packing and also give a first insight into their complexation behavior. These facets comprise the synthesis of cycle **1c**, which differs from the known **1b** by its tetrahydropyranyl (THP) protecting groups at the four hydroxy functions, as well as the complexation of both bipy units in the cycles **1a** and **1c** with $[Ru(bipy)_2]$ fragments. We also report the X-ray crystal structure determinations of cycles **1a**, **1c**, and a model Ru complex and initial experiments on the deprotection of the THP-protected alcohol functions of complexed **1c**.

[a] Prof. Dr. A. D. Schlüter, Priv.-Doz. Dr. D. Lentz, Dr. O. Henze, Dr. A. Schäfer, Dr. P. Franke
Freie Universität Berlin, Institut für Chemie
Takustrasse 3, 14195 Berlin (Germany)
Fax: (+49) 30-838-53357
E-mail: adschlue@chemie.fu-berlin.de

Results and Discussion

Synthesis of cycle 1c: To enter the relatively complex field described in the introduction, it was considered advisable to have a few cycles available which do not differ in ring size but in their substitution pattern. This pattern plays an important role with regard to various properties of the cycle, for example, solubility, aggregation, and potential for chemical

  0947-6539/02/0802-0357 $ 17.50+.50/0

modification. Cycle **1c** complements its analogues **1a** and **1b** specifically in the ease with which the deprotection of its alcohol functions should proceed,[14] the necessary first step for further chemical modification. Cycle **1c** was therefore considered an important target structure and synthesized in analogy to the known cycles **1a** and **1b** (Scheme 1). The key

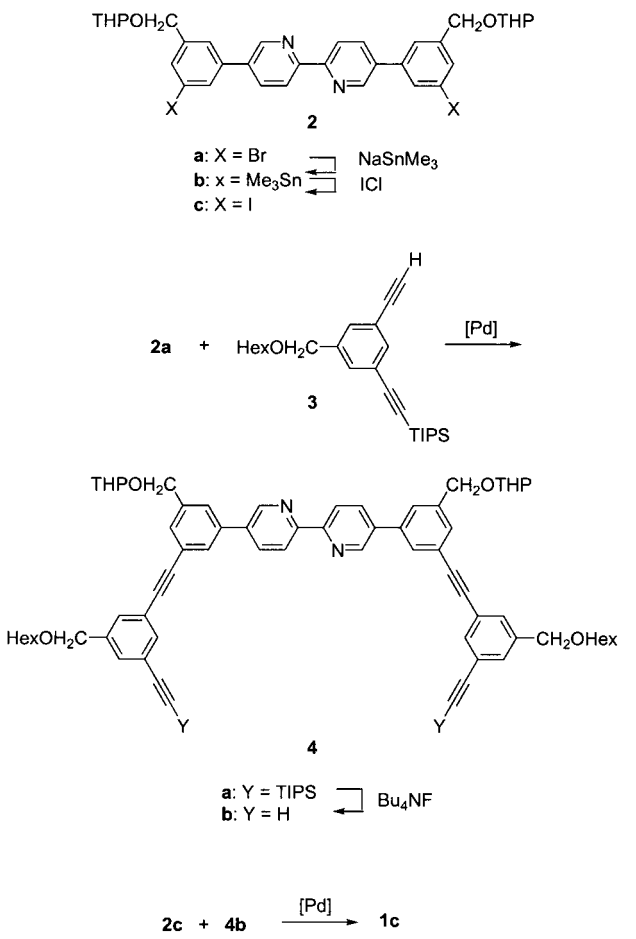

Scheme 1.

building block **2a**[15] served as the starting material for both components, that is, **2c** and **4b**, with which the ring closure was achieved. Dibromide **2a** was not used directly for this purpose (instead of **2c**) because diiodides generally furnish higher yields in related cyclization reactions. This can go as far as to render a cyclization involving diiodides possible that does not occur at all with the corresponding dibromides.[16]

The conversion of dibromide **2a** into its diiodo counterpart **2c** was achieved by consecutive nucleophilic stannylation[17] and iododestannylation[17] steps passing through distannyl **2b**. The bisacetylene counterpart **4b** was obtained by reacting **2a** with the tri(isopropyl)silyl (TIPS)-protected building block **3**,[1] followed by deprotection of the acetylenic functions with tetrabutylammonium fluoride (TBAF). The ring closure was carried out under high dilution conditions by means of a Sonogashira–Hagihara-type reaction.[18] Cycle **1c** was obtained in a yield of 14% on the 100–200 mg scale after purification by preparative gel-permeation chromatography. The rest of the material was partially insoluble and not investigated further. The reasons for this low yield are not yet known. Yields for cycle formation from related conformationally rigid AA- and BB-type building blocks range between 25 and 40%,[1, 2, 19–21] or even higher in some special cases.[4, 20, 22] For macrocycles of AB-type compounds, where only one C–C bond-formation step is required, yields of 70% and more have been observed.[16]

Cycle **1c** could not be obtained as analytically pure material; however, it was unambiguously characterized by NMR spectroscopy, mass spectrometry, and X-ray diffraction of single crystals (see below). Both the ^{1}H and ^{13}C NMR spectra are complicated by the large number of diastereomers that result from the chiral centers introduced through the THP groups.

Complexation of model compound 5 and cycle 1a with [Ru(bipy)Cl$_2$]: Ru complexes of all kinds of bipyridine ligands have been reported.[23, 24] Compound *rac*-**6** is a standard reagent for this purpose and was therefore used in the present study.[25] Complexation of **5**, which conveniently gave *rac*-**7** in ethanol/water (50:50) (Scheme 2), was less complex than for

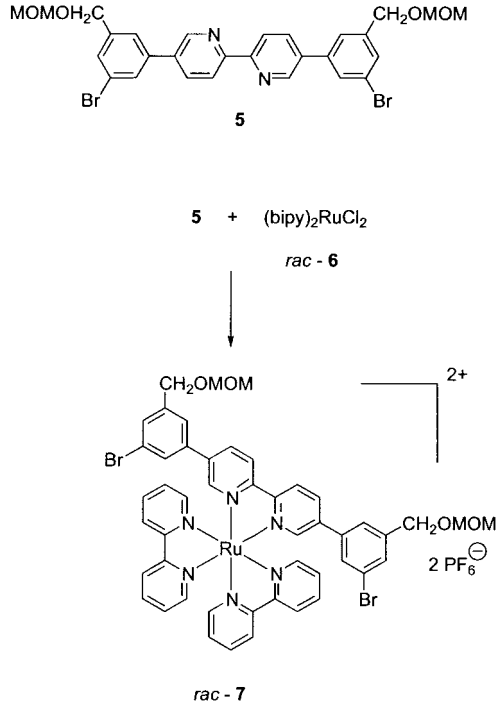

Scheme 2.

cycle **1a** (Scheme 3). In both cases (**1a** and **1c**), the expected color change from purple for *rac*-**6** to red/orange for the complex was not observed, although various solvent combinations were tested. Finally, the cycle was heated to 100 °C in ethylene glycol, and dioxane was added until a 3:1 (v/v) proportion of the solvents was reached. Subsequently, two equivalents of *rac*-**6** were added and the resulting mixture refluxed for 12 h. After removal of the solvent, the remaining

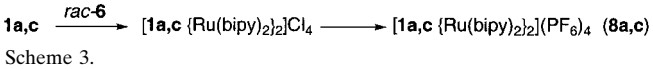

Scheme 3.

0947-6539/02/0802-0358 $ 17.50+.50/0 *Chem. Eur. J.* **2002**, *8*, No. 2

mass was separated by chromatography through silica gel under specific conditions that involved the use of aqueous ammonium chloride, nitromethane, and methanol (see the Experimental Section). The obtained complex, **8a**, contained chlorides as counterions, which were exchanged by the addition of excess ammonium hexafluorophosphate to a methanol solution of the chloride. The resulting precipitate was filtered off and carefully washed with water. Complex **8a** is soluble in acetonitrile, pyridine, and acetone.

Complex *rac*-**7** was characterized by NMR spectroscopy, FAB-mass spectrometry, correct data from combustion analysis, and X-ray crystal structure analysis (see below). Complex **8a** was characterized by NMR spectroscopy (see below) and matrix-assisted laser-desorption ionization time-of-flight mass spectrometry (MALDI-TOF).

MALDI-TOF and NMR-spectroscopic characterization of complex 8a: Complex **8a** was investigated by MALDI-TOF and NMR spectroscopy (500 MHz). The mass spectrum was recorded in a dithranol matrix and shows a number of characteristic signals with regard to both the mass they correspond to and the isotope patterns (Figure 1). Both features show unambiguously that **8a** contains two [Ru(bipy)$_2$] fragments. Especially characteristic is the virtually identical mass difference between the signals at $m/z = 2581$, 2436, 2291, and 2149 that proves the step-wise fragmentation of the four PF_6^- counterions. The assignment of these and the other signals is summarized in Table 1. For this assignment, some proton- and electron-transfer processes were assumed that are likely to occur under the applied conditions. The experimental isotopic distribution was compared to that calculated for all signals and was found to be in good agreement. Table 2 contains this comparison for the signal at $m/z = 2581$; see the insert in Figure 1.

The dinuclear complex **8a** has two enantiomeric forms (Λ,Λ and Δ,Δ) and one *meso* form (Λ,Δ)(Figure 2). Its

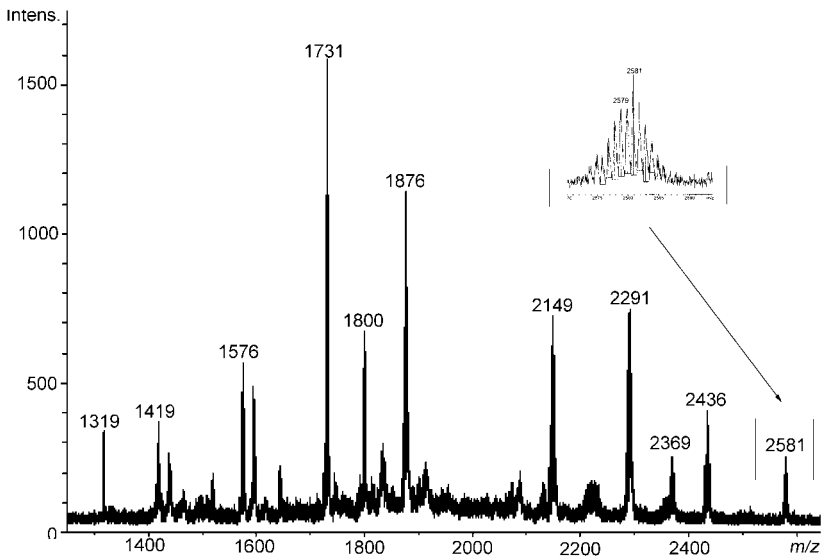

Figure 1. MALDI-TOF mass spectrum (dithranol matrix) of Ru complex **8a**. For the fragmentation pattern, see Table 1. Insert: Expanded and amplified isotope pattern of the MALDI-TOF mass spectral signal of the Ru complex **8a** at $m/z = 2581$ $[M+H-PF_6]^+$. For a comparison of the observed and calculated intensities, see Table 2.

Table 1. Assignments and fragmentation of some MALDI-TOF mass spectrum signals of complex **8a**.

Mass	Assigned formula	Fragmentation
2581	$C_{132}H_{125}N_{12}O_4Ru_2P_3F_{18}$	$[M+H-PF_6]^+$
2436	$C_{132}H_{125}N_{12}O_4Ru_2P_2F_{12}$	$[M+H-2PF_6]^+$
2291	$C_{132}H_{125}N_{12}O_4Ru_2PF_6$	$[M+H-3PF_6]^+$
2149	$C_{132}H_{128}N_{12}O_4Ru_2$	$[M+4H-4PF_6]^+$
1876	$C_{112}H_{108}N_8O_4RuPF_6$	$[M-3PF_6-Ru-2bipy]^+$
1731	$C_{112}H_{108}N_8O_4Ru$	$[M-4PF_6-Ru-2bipy]^+$
1575	$C_{102}H_{101}N_6O_4Ru$	$[M+H-4PF_6-Ru-3bipy]^+$
1419	$C_{92}H_{92}N_4O_4Ru$	$[M-4PF_6-Ru-4bipy]^+$
1319	$C_{92}H_{93}N_4O_4$	$[M+H-4PF_6-2Ru-4bipy]^+$

Table 2. Calculated and experimental isotope intensities for the MALDI-TOF signal of complex **8a** at $m/z = 2581$.

Mass	Calcd	Found
2576	28	38
2577	39	50
2578	58	64
2579	73	77
2580	89	73
2581	100	100
2582	92	78
2583	82	60
2584	62	48

^{1}H NMR spectrum is therefore quite complex (Figure 3). Four sets of signals are observed for the bipy ligands and two sets for those of the cycle. The assignment of these sets was possible by means of HMQC, COSY, and HOHAHA experiments including the ^3J couplings. Some of the signal sets are rather complex, for example, H10 and H11, while for others, such as H6, only two singlets appear. H10 appears as four doublets and H11 as four doublets of doublets. This spin system is produced by the different pyridine subunits of the four bipy ligands (two for the pair of enantiomers and two for the *meso* stereoisomer). The protons of the cycle are either homotopic (Λ,Λ and $\Delta\Delta$) or enantiotopic (Λ,Δ). H6 appears as two singlets, one of which stems from the pair of enantiomers and the other one from the *meso* form. As expected, the ratio of these two forms is 1:1, as is indicated, for example, by the intensity ratio of the two singlets.

Crystal structures of cycles 1a, 1c, and complex *rac*-7: Cycle **1a**·$3C_6H_6$ crystallizes in the triclinic space group $P\bar{1}$ with half a molecule in the asymmetric unit. The molecular structure and the positions of the solvent molecules are depicted in Figure 4a. In the macrocycle, two of its hexoxymethyl sidechains and two benzene

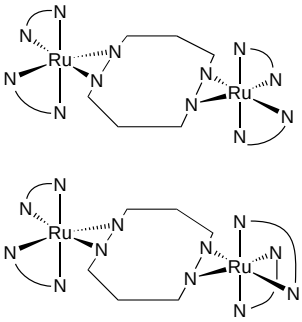

Figure 2. Cartoon representation of two stereoisomeric forms of **8a**: Λ,Δ (top), Λ,Λ (bottom).

solvent molecules are ordered, and the other two hexoxymethyl chains and the remaining benzene molecule possess great positional freedom, as expressed by the larger thermal ellipsoids. Almost all atoms of the macrocycle and the carbon atoms of the ordered sidechains are in one plane, whereas the disordered sidechains are dangling out of this plane. The bipy units are turned out of the plane with torsional angles of $\approx 39^\circ$ (Figure 4b). The data does not allow an unambiguous assignment of the bipy nitrogen atoms which may be disordered.

Figure 5 shows a view of the packing diagram of **1a** along the crystallographic *a* axis. The individual macrocycles are only overlapping at the bipyridine units which have the shortest interatomic distances of 3.67 Å between C34 of two neighboring molecules (not shown). This results in channels parallel to the *a* axis. The channels are filled by two hexyl sidechains of two adjacent macrocycles and one benzene molecule. As can be seen from the large thermal ellipsoids of this part of the molecule, there is still some nonoccupied volume which, however, is too small for additional solvent molecules. The remaining hexyl sidechains are directed parallel to the *c* axis within the plane of the macrocycle; this creates further channels parallel to the *a* axis that are effectively filled by benzene molecules. All in all, this results in an effective packing of the molecule together with the three benzene solvate molecules.

Cycle **1c**·4$CHCl_3$ also crystallizes in the triclinic space group $P\bar{1}$. The asymmetric unit consists of half a molecule of

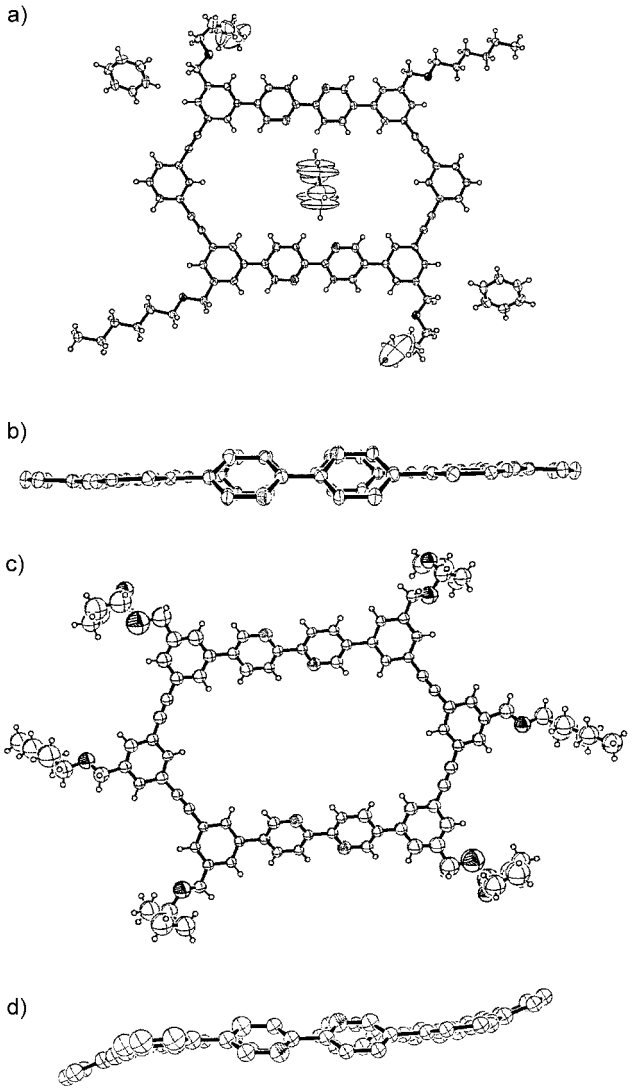

Figure 4. Molecular structures (ORTEP[34]) of **1a** and **1c**. Top view (a,c) and side view (b,d) of the cycles **1a** (a,b) and **1c** (c,d).

1c and two chloroform solvate molecules. The complete molecule is generated by a crystallographic inversion center. The molecular structure of cycle **1c** and the positions of the ordered solvent molecules are depicted in Figure 4c. Although the crystal was mounted at low temperature and the data were collected at -110°C, the sidechains and the THP rings are very flexible and the solvent molecules have some rotational and positional freedom, as can be seen from the much larger thermal ellipsoids of these moieties compared to the macrocycle. Furthermore, only one of the two solvent molecules could be located in the difference Fourier map and refined, whereas the other one gives only weak peaks in the differ-

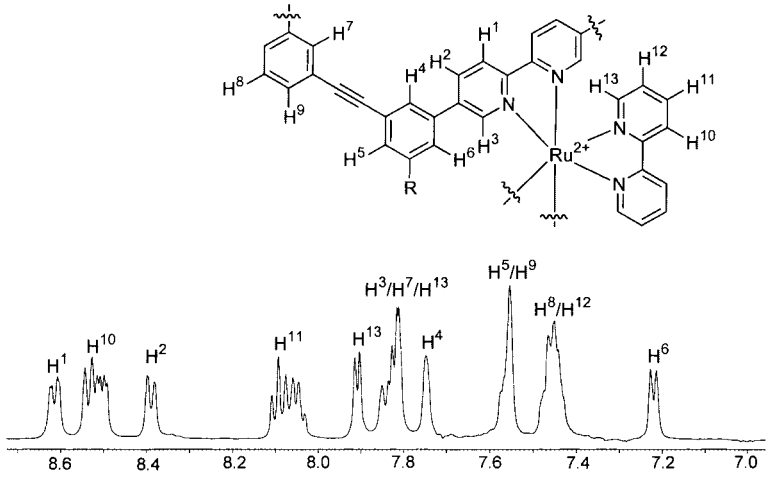

Figure 3. ^{1}H NMR spectrum (CH_3CN, 20 °C, 500 MHz) of the stereoisomeric mixture of **8a** with signal assignment.

0947-6539/02/0802-0360 $ 17.50+.50/0 *Chem. Eur. J.* **2002**, *8*, No. 2

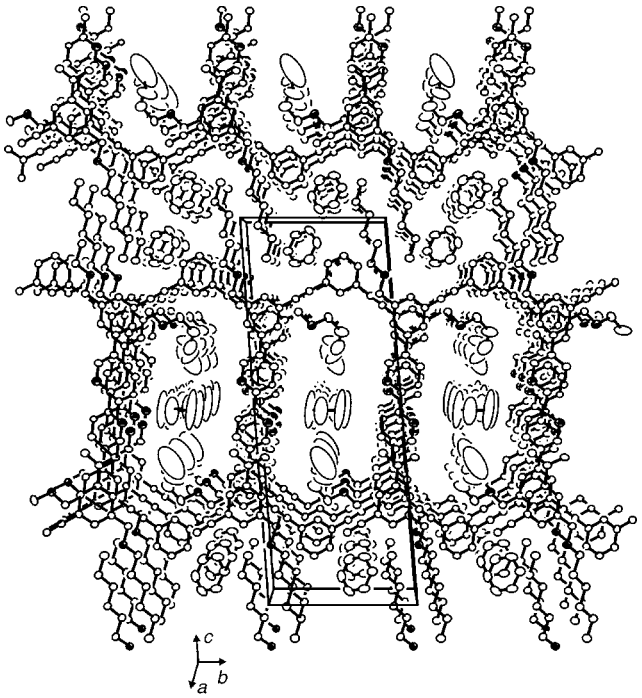

Figure 5. Packing diagram (ORTEP[34]) of **1a**. View along the crystallographic *a* axis.

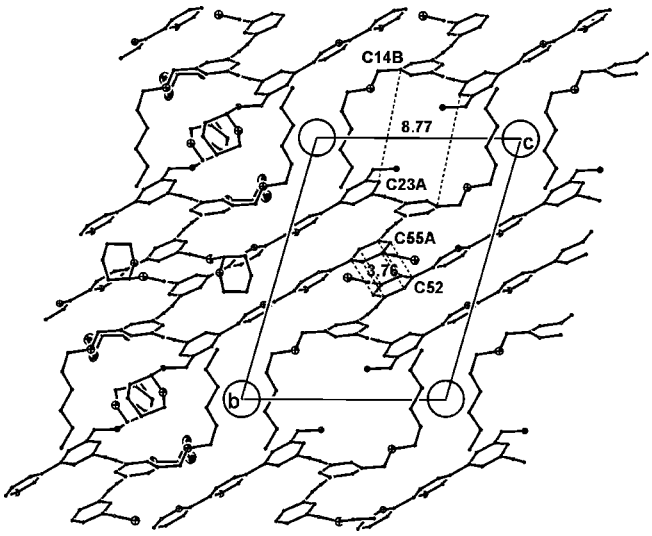

Figure 6. Packing diagram of **1c** (ORTEP[34]). View along the crystallographic *a* axis. The left-hand side of the drawing shows the molecules, including the THP sidechains and the chloroform solvate molecules. These are omitted on the right-hand side for clarity. The positions of the disordered solvent molecules in 0.500, 0.501, 0.510, and 0.511 are indicated by the large circles. The molecule labeled A is generated by the symmetry operation $1-x, 1-y, 1-z$. The molecule label B is generated from A by the symmetry operation $x, 1-y, z$.

ence Fourier map. An analysis of the structure with PLATON[26] resulted in solvent-accessible areas of 189 Å^3 centered around 0.501. The program SQUEEZE in the PLATON[26] package was used to calculate and correct for electron density (65 e$^-$) identified in a solvent-accessible area. As $CHCl_3$ was used as the solvent, and it possesses 58 e$^-$, we can assume that this area is occupied by an additional disordered chloroform molecule. By the use of the corrected *hkl* file, the refinement converged at $R1 = 0.204$, whereas the uncorrected data resulted in $R1 = 0.243$. The still unsatisfactory *R* values are probably the result of disorder of the THP units which consist of various stereoisomers, and because the crystal shows only extremely weak diffraction for 2θ values above 35°. Therefore, all atoms except chlorine had to be refined isotropically to maintain a reasonable reflection/parameter ratio. Again, it was not possible to differentiate between carbon and nitrogen atoms in the bipy ring. The molecular structure of **1c** is depicted in Figure 4c,d. The cycle **1c** attains an S-shaped conformation (Figure 4d), whereby the bipy units are less tilted out of planarity than those in **1a**. Figure 6 shows the packing diagram with a view along the crystallographic *a* axis. The plane of the macrocycles is oriented roughly perpendicular to 111. The ordered chloroform molecules fill holes in such a way that the hydrogen atom is directed towards the nitrogen atom N2 of one bipyridine ring (normalized distance H1L···N2′ 2.35,[27, 28] symmetry operation to generate N2′: $x, y-1, +z$). The second strongly disordered solvate molecule is centered around 0.500, as indicated by the large circles. Only the left-hand part of Figure 6 shows the THP substituents and the chloroform solvate molecules; they are omitted in the right-hand side for clarity. Two THP substituents of adjacent molecules are embedded between two antiparallel hexyl sidechains of the same molecules. The other THP sidechains are dangling into the holes of the macrocycles. As can be seen from the disorder of one of the solvate molecules, the packing in **1c** is less effective than in **1a**. In addition, there might be a misfit of the packing within the THP sidechains as a result of the presence of several stereoisomers.

Figure 7 exhibits a simplified packing diagram of the cycles **1a**–**1c** with a view almost perpendicular to the ring planes. All chains and solvent molecules have been omitted for clarity. The previously published structure of **1b**[1] is included in Figure 7 for comparison. All three structures may be regarded as composed of layers. Each of these layers is defined by the macrocycles within one plane. The rings within one layer are labeled by the same color. The different colors allow an easy recognition of the principal motifs and the stacking. However, this does not imply that the molecules are crystallographically different. All three cycles form structures with "channels"[29] perpendicular to the plane of the cycle. The sides overlap, whereby subsequent layers are shifted towards each other and most likely assume the following sequences **1a**: AB, **1b**: ABC, and **1c**: ABCD. The packing of **1a** differs from that of the other cycles by the fact that the overlap does not exist in all directions. This gives rise to the formation of new layers perpendicular to those in which the cycles lie (see Figure 7). Although all three macrocycles have, in principal, the same shape, their packing is completely different because of the different sidechains and solvate molecules which seem to play a role in the stabilization of the lattice. Compound *rac*-**7** crystallizes in the monclinic, centrosymmetric space group $P2_1/c$, and contains the anatiomeric forms in the unit cell. The molecular structure of 7 is depicted in Figure 8. The bipy unit is almost planar (angle N1-C1-C2-N2: $-3.4(4)°$), whereas the phenyl substituents are tilted by about 30°. The N1-C1-C2

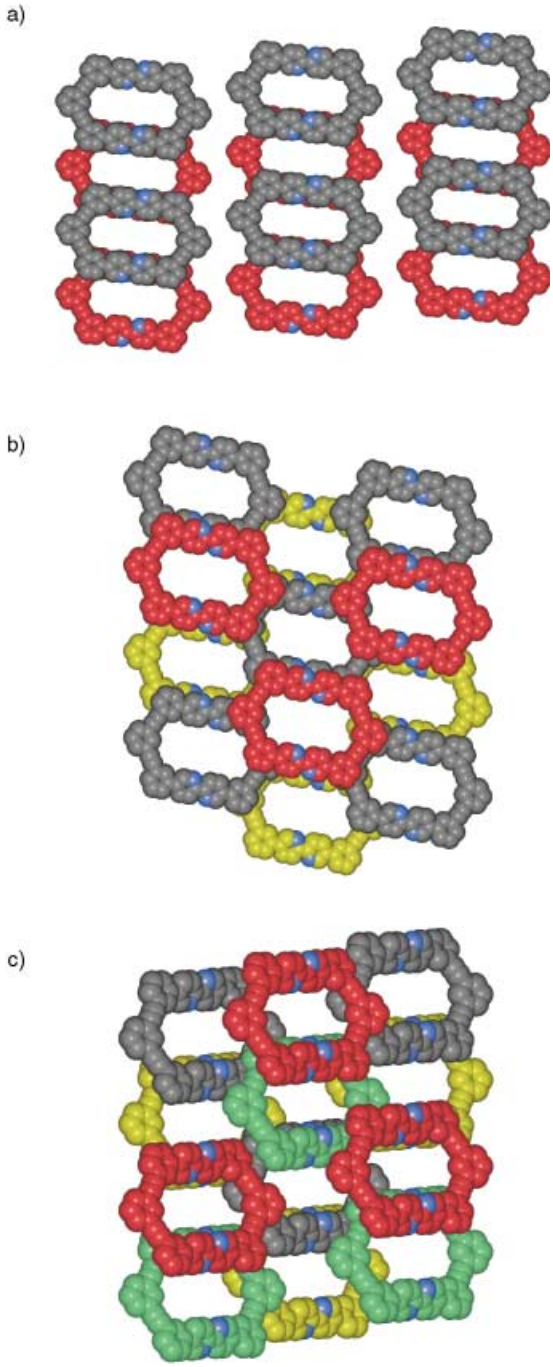

Figure 7. Schematic representation of the packing of the cycles a) **1a**, b) **1b**, and c) **1c** in the crystals. The sidechains and entrapped solvent molecules have been omitted for clarity. View perpendicular to the plane of the cycles. Molecules within the same layer are labeled with the same color code for easier recognition of the motifs and the stacking.

angle is 114.8(3)°, which causes the complexed unit to bend slightly out of linearity.

Preliminary experiment aimed at the deprotection of the THP groups of complexed cycle 8c: As mentioned in the introduction, cycle **1c**, with its THP-protected alcohol functions was prepared in order to use these functions for further modification of the cycle's periphery. However, treatment of **1c** with acid did not lead to any deprotection but rather to

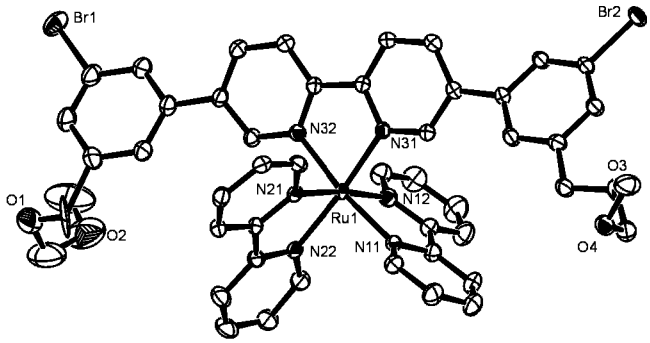

Figure 8. Molecular structure (ORTEP[34]) of *rac*-**7c**.

precipitation of the cycle, presumably through salt formation between the acid and bipy. At this point we cannot exclude that deprotection actually took place and that the tetrol formed is insoluble. The bipy units were therefore blocked by complexation with the $[Ru(bipy)_2]$ fragment, as described for cycle **1a**. Treatment of complex **8c** (which was not fully characterized and is therefore not described in the Experimental Section but in Ref. [30]) with 2% HCl in methanol was sufficient to cleave off the THP group. This was proven by the disappearance of the respective signals in the proton NMR spectrum and the concomitant simplification of the benzylic proton signals, which in the unprotected form do not have stereocenters in close proximity anymore. The FAB mass spectrum shows the expected molecular ion peak at $m/z = 2471$ $[M - PF_6]^+$.[30]

Experimental Section

General: All reagents and compound *rac*-**6** were purchased from Aldrich or Acros and used without further purification. Compounds **2a**,[15] **3**,[1] **5**,[1] and $NaSn(CH_3)_3$[17] were prepared according to the literature. Melting points: Büchi SMP510 (open capillaries, uncorrected values). NMR: Bruker AC250, AM270, AMX500 (^{1}H: $CDCl_3$ at $\delta = 7.24$, ^{13}C: $CDCl_3$ at $\delta = 77.00$ as internal standards, 20°C). MS: Perkin–Elmer Varian MAT711, electron-impact (EI) mode. Elemental analyses: Perkin–Elmer EA240. Column chromatography: Merck silica gel 60, 0.040–0.063 mm (230–400 mesh).

5,5′-Bis-[3-(tetrahydropyran-2-yloxymethyl)-5-trimethyl-stannylphenyl]-[2,2′]bipyridinyl (2b): A suspension of **2a** (1.5 g, 2.2 mmol) in DME (10 mL) was added over a period of 20 min to a solution of $NaSn(CH_3)_3$ in DME (30 mL), prepared from Na (1.9 g) and $ClSn(CH_3)_3$ (5.16 g, 25.9 mmol). After stirring for 20 h at room temperature, the solvent was removed under reduced pressure and the residual material was purified by chromatography through silica gel (ethyl acetate/hexane 1:6) to give 1.21 g (65.1%) of **2b** as a colorless powder. $R_f = 0.29$ (ethyl acetate/hexane 1:3); m.p. 126°C; ^{1}H NMR ($CDCl_3$, 250 MHz): $\delta = 0.30$ (s, 18H; $Sn(CH_3)_3$), 1.45–1.90 (m, 12H; THP), 3.48–3.58 (m, 2H; THP), 3.82–3.98 (m, 2H; THP), 4.53 (d, $^2J = 13$ Hz, 2H; benzyl-H), 4.72 (s, 2H; THP), 4.82 (d, $^2J = 13$ Hz, 2H; benzyl-H), 7.49 (s, 2H; phenyl-H), 7.55 (s, 2H; phenyl-H), 7.61 (s, 2H; phenyl-H), 7.98 (dd, $^3J = 8$ Hz, $^4J = 2$ Hz, 2H; py-H), 8.49 (d, $^3J = 8$ Hz, 2H; py-H), 8.89 (d, $^4J = 2$ Hz, 2H; py-H); ^{13}C NMR ($CDCl_3$, 63 MHz): $\delta = -9.4$, 19.4, 25.5, 30.6, 62.2, 68.8, 97.9, 120.9, 126.7, 133.6, 135.1, 135.4, 136.7, 137.3, 138.5, 143.6, 147.8, 154.6; MS (EI): m/z (%): 862 (45.7), 847 (100); elemental analysis calcd (%) for $C_{42}H_{60}N_2O_2Sn_2$ (860.23): C 55.85, H 5.85, N 3.25; found: C 55.75, H 5.98, N 2.84.

5,5′-Bis-[3-iod-5-(tetrahydropyran-2-yloxymethyl)phenyl]-[2,2′]bipyridinyl (2c): I_2 (0.72 g, 2.8 mmol) was added over a period of 15 min at room temperature to a solution of **2b** (1.2 g, 1.4 mmol) in $CHCl_3$ (30 mL). After stirring for 2 h, a saturated solution of KF (20 mL) was added. The resulting mixture was made alkaline with potassium carbonate, and the phases were

  0947-6539/02/0802-0362 $ 17.50+.50/0 *Chem. Eur. J.* **2002**, *8*, No. 2

separated. The aqueous phase was washed with $CHCl_3$ (2×30 mL). The combined organic phase was washed once more with a saturated solution of KF (20 mL) and then with a saturated sodium thiosulfate solution (20 mL). The organic phase was dried over $MgSO_4$, the solvent was removed, and the resulting oil purified by chromatography through silica gel (ethyl acetate/hexane 1:3) to give 1.1 g (97%) of **2c** as a white powder. $R_f = 0.37$ (ethyl acetate/hexane 1:3); m.p. 178 °C; ^{1}H NMR ($CDCl_3$, 250 MHz): $\delta =$ 1.50–1.95 (m, 12H; THP), 3.50–3.60 (m, 2H; THP), 3.89 (mc, 2H; THP), 4.50 (d, $^2J = 13$ Hz, 2H; benzyl-H), 4.69 (dd, 2H; THP), 4.82 (d, $^2J = 13$ Hz, 2H; benzyl-H), 7.60 (s, 2H; phenyl-H), 7.75 (s, 2H; phenyl-H), 7.91 (s, 2H; phenyl-H), 7.99 (dd, $^3J = 8$ Hz, $^4J = 2$ Hz, 2H; py-H), 8.51 (d, $^3J = 8$ Hz, 2H; py-H), 8.87 (d, $^4J = 2$ Hz, 2H; py-H); ^{13}C NMR ($CDCl_3$, 63 MHz): $\delta = 19.2$, 25.3, 30.4, 62.1, 66.9, 67.6, 95.0, 98.0, 120.9, 125.5, 134.9, 135.1, 136.1, 139.6, 141.4, 147.4, 147.5, 154.8; MS (EI): *m*/*z* (%): 788 (100), 688 (70.3); elemental analysis calcd (%) for $C_{34}H_{34}N_2O_4I_2$ (800.47): C 51.79, H 4.3,5 N 3.55; found: C 51.70, H 4.32, N 3.35.

5,5′-Bis-[3-(3-hexyloxymethyl-5-triisopropylsilylethinylphenylethinyl)-5-(tetrahydropyran-2-yloxymethyl)phenyl]-[2,2′]bipyridinyl (4a): A heavy-walled flask was charged with **3** (3.4 g, 8.6 mmol), **2a** (2.0 g, 2.9 mmol), $[Pd(PPh_3)_4]$ (0.04 equiv), CuI (0.04 equiv), dry triethylamine (40 mL), and toluene (20 mL). The flask was then evacuated and backfilled with nitrogen three times and sealed with a Teflon screw cap, and the solution was stirred at 80 °C for 24 h. Then the solvent was removed, and the residual material was purified by column chromatography through silica gel (ethyl acetate/hexane 1:3) to give 3.3 g (75%) of **4a** as a light yellow oil. $R_f = 0.23$ (ethyl acetate/hexane 1:3); ^{1}H NMR ($CDCl_3$, 500 MHz): $\delta = 0.88$ (t, 6H; CH_3), 1.12 (s, 42H; $Si(C_3H_7)_3$), 1.29 (mc, 8H; hexyl-CH_2), 1.37 (mc, 4H; hexyl-CH_2), 1.52–1.66 (m, 10H; hexyl-CH_2/THP), 1.72 (mc, 2H; THP), 1.77 (mc, 2H; THP), 1.89 (mc, 2H; THP), 3.47 (t, 4H; α-CH_2), 3.58 (mc, 2H; THP), 3.93 (mc, 2H; THP), 4.45 (s, 2H; benzyl-CH_2), 4.57 (d, $^2J = 13$ Hz, 4H; benzyl-CH_2), 4.77 (s, 2H, THP), 4.88 (d, $^2J = 13$ Hz, 2H; benzyl-H), 7.42 (s, 2H; phenyl-H), 7.49 (s, 2H; phenyl-H), 7.58 (s, 2H; phenyl-H) 7.60 (s, 2H; phenyl-H) 7.62 (s, 2H; phenyl-H) 7.73 (s, 2H; phenyl-H), 8.05 (d, $^3J = 8$ Hz, 2H; py-H), 8.52 (d, $^3J = 8$ Hz, 2H; py-H), 8.94 (s, 2H; py-H); ^{13}C NMR ($CDCl_3$, 126 MHz): $\delta = 11.0$, 11.2, 14.0, 18.6, 19.2, 22.6, 25.3, 25.8, 29.6, 30.4, 31.6, 62.1, 68.1, 70.7, 71.8, 89.1, 89.3, 91.3, 97.9, 105.9, 121.0, 123.1, 123.9, 123.9, 126.3, 129.2, 130.4, 130.9, 134.1, 135.2, 135.5, 137.9, 139.3, 139.7, 147.6, 154.8; MS (EI, 80 eV): *m*/*z* (%): 1326 (4.9), 1283 (100); elemental analysis calcd (%) for $C_{86}H_{112}N_2O_6Si_2$ (1326.02): C 77.90, H 8.51, N 2.11; found: C 77.67, H 8.26, N 2.00.

5,5′-Bis-[3-(3-ethinyl-5-hexyloxymethylphenylethinyl)-5-(tetrahydropyran-2-yloxymethyl)phenyl]-[2,2′]bipyridinyl (4b): Tetrabutylammonium fluoride trihydrate (1.7 g, 5.3 mmol) was added to a stirred solution of **4a** (3.2 g, 2.4 mmol) in THF (50 mL). After complete consumption of the starting material (1 h), the reaction mixture was diluted with diethyl ether (100 mL) and water (80 mL). The phases were separated. The aqueous phase was washed with diethyl ether (50 mL), and the combined organic phase was washed with water (50 mL). The organic phase was dried over $MgSO_4$, the solvent removed, and the residual material purified by column chromatography through silica gel (ethyl acetate/hexane 1:3) to give 2.2 g (92%) of **4b** as a light yellow oil. $R_f = 0.07$(ethyl acetate/hexane 1:3); ^{1}H NMR ($CDCl_3$, 500 MHz): $\delta = 0.86$ (t, 6H; CH_3), 1.29 (mc, 8H; hexyl-CH_2), 1.36 (mc, 4H; hexyl-CH_2), 1.60 (mc, 10H; hexyl-CH_2/THP), 1.70 (mc, 2H; THP), 1.76 (mc, 2H; THP), 1.86 (mc, 2H; THP), 3.10 (s, 2H; acetylene-H), 3.45 (t, 4H; α-CH_2), 3.57 (mc, 2H; THP), 3.92 (mc, 2H; THP), 4.44 (s, 2H; benzyl-CH_2), 4.55 (d, $^2J = 13$ Hz, 4H; benzyl-CH_2), 4.76 (s, 2H, THP), 4.86 (d, $^2J = 13$ Hz, 2H; benzyl-H), 7.39 (s, 2H; phenyl-H), 7.49 (s, 2H; phenyl-H), 7.55 (s, 2H; phenyl-H) 7.58 (s, 2H; phenyl-H) 7.60 (s, 2H; phenyl-H) 7.69 (s, 2H; phenyl-H), 8.01 (d, $^3J = 9$ Hz, 2H; py-H), 8.50 (d, $^3J = 9$ Hz, 2H; py-H), 8.91 (s, 2H; py-H); ^{13}C NMR ($CDCl_3$, 126 MHz): $\delta = 14.0$, 19.2, 22.5, 25.3, 25.7, 29.6, 30.4, 31.6, 62.1, 68.1, 70.7, 71.7, 77.8, 82.6, 88.9, 89.5, 97.9, 120.9, 122.4, 123.3, 123.8, 126.3, 129.1, 130.3, 130.8, 130.9, 134.0, 135.2, 135.4, 137.8, 139.4, 139.6, 147.5, 154.7; MS (FAB): *m*/*z* (%): 1013 (11.3); elemental analysis calcd (%) for $C_{68}H_{72}N_2O_6$ (1013.33): C 80.60, H 7.16, N 2.76; found: C 80.48, H 7.08, N 2.70.

Macrocycle 1c: A solution of **4b** (730 mg, 0.72 mmol) and **2c** (570 mg, 0.72 mmol) in a mixture of triethylamine (250 mL) and toluene (250 mL) was carefully degassed. After adding $Pd[(PPh_3)_4]$ (33 mg, 0.04 equiv) and copper(I) iodide (5.5 mg, 0.04 equiv), this mixture was stirred under nitrogen at 60 °C for 4 d and then at 95 °C for 24 h. After cooling, the orange suspension was treated with a solution of KCN (300 mg) in water (100 mL); the color changed to white. The mixture was then filtered and the insoluble residue was washed with toluene (2×50 mL). The phases were separated. The aqueous phase was washed with toluene (50 mL) and the combined organic phase with water (100 mL). The organic phase was dried over $MgSO_4$ and the solvent removed. Purification of the residue by GPC gave 160 mg (14%) of cycle **1c**. (M.p. under investigation). ^{1}H NMR ($CDCl_3$, 500 MHz): $\delta = 0.90$ (t, 6H; CH_3), 1.32 (mc, 8H; hexyl-CH_2), 1.40 (mc, 4H; hexyl-CH_2), 1.52–1.82 (m, 24H; THP), 1.89–1.96 (m, 4H; β-CH_2), 3.51 (t, 4H; α-CH_2), 3.54–3.62 (m, 4H; THP), 3.95 (mc, 4H; THP), 4.49 (s, 4H; benzyl-CH_2), 4.54 (d, $^2J = 13$ Hz, 4H; benzyl-CH_2), 4.78 (dd, $^3J = 2$ Hz, 4H; THP), 4.82 (d, $^2J = 13$ Hz, 4H; benzyl-H), 7.45 (s, 4H; phenyl-H), 7.49 (s, 4H; phenyl-H), 7.52 (s, 4H; phenyl-H) 7.65 (s, 4H; phenyl-H), 7.67 (s, 2H; phenyl-H), 7.98 (dd, $^3J = 8$ Hz, $^4J = 2$ Hz, 4H; phenyl-H), 8.46 (d, $^3J = 8$ Hz, 4H; py-H), 8.88 (s, 4H; py-H); ^{13}C NMR ($CDCl_3$, 126 MHz): $\delta = 14.1$, 19.3, 22.6, 25.4, 25.8, 29.7, 30.5, 31.7, 62.2, 68.2, 70.8, 72.0, 89.2, 89.6, 97.9, 121.0, 123.4, 123.9, 125.8, 129.3, 130.1, 130.2, 134.3, 135.0, 137.5, 139.4, 139.5, 139.7, 147.3, 154.5; MS (FAB): *m*/*z* (%): 1547 (0.3).

***rac*-7**: A stirred solution of **5** (139 mg, 0.2 mmol) and $[Ru(bpy)_2Cl_2] \cdot 2H_2O$ (104 mg, 0.2 mmol) in ethanol (3.8 mL) and H_2O (1.2 mL) was refluxed for 24 h. Then the solvent was removed, and the residual orange material purified by column chromatography through silica gel (methanol/2 M NH_4Cl/nitromethane 7:2:1). The combined orange fractions were diluted with CH_2Cl_2, the organic phase was separated, and the solvent removed. The orange residue was dissolved in methanol (2 mL) and added to a solution of NH_4PF_6 (200 mg) in H_2O (2 mL). The precipitated solid was separated by filtration, washed with H_2O (4×2 mL), and dried in a vacuum to give 85 mg (32%) of *rac*-**7** as an orange solid. ^{1}H NMR (DMSO/$CDCl_3$ 50:50, 250 MHz): $\delta = 3.29$ (s, 6H; CH_3), 4.49 (s, 4H; CH_2), 4.62 (s, 4H; CH_2), 7.29 (s, 2H; phenyl-H), 7.45–7.56 (m, 6H; phenyl-H, py-H), 7.62 (d, $^4J = 2$ Hz, 2H; py-H), 7.79 (d, $^3J = 5$ Hz, 2H; py-H), 7.88 (d, $^3J = 5$ Hz, 2H; py-H), 8.10 (dd, $^3J = 7$ Hz; 2H; py-H), 8.14 (dd, $^3J = 7$ Hz, 2H; py-H), 8.42 (dd, $^3J = 9$ Hz, $^4J = 2$ Hz, 2H; py-H), 8.75 (d, $^3J = 7$ Hz, 2H; py- H), 8.80 (d, $^3J = 7$ Hz, 2H; py- H), 8.90 (d, $^3J = 9$ Hz, 2H; py- H); ^{13}C NMR (DMSO/$CDCl_3$ 50:50, 63 MHz): $\delta = 54.8$, 67.1, 95.3, 122.5, 124.3, 127.4, 127.6, 128.4, 130.8, 135.6, 136.2, 137.5, 137.7, 141.5, 148.0, 151.4, 155.2, 156.1, 156.6; MS (FAB +): *m*/*z* (%): 1173 (11.8) $[M - PF_6]^+$; elemental analysis calcd (%) for $C_{48}H_{42}Br_2F_{12}N_6O_4P_2Ru$ (1317.70): C 43.75, H 3.21, N 6.38; found: C 43.33, H 3.11, N 6.16.

[1a{Ru(bpy)$_2$}$_2$](PF$_6$)$_4$ (8a): A stirred solution of **1a** (40 mg, 0.03 mmol) and $[Ru(bpy)_2Cl_2] \cdot 2H_2O$ (21.6 mg, 0.06 mmol) in dioxane (12 mL) and ethylene glycol (4 mL) was refluxed for 24 h. The solvent was removed, and the residual orange material purified by column chromatography through silica gel (methanol/2 M NH_4Cl/nitromethane 7:2:1). The combined orange fractions were diluted with $CHCl_3$, the organic phase was separated, and the solvent removed. The orange residue was then dissolved with methanol (2 mL) and added to a solution of NH_4PF_6 (200 mg) in H_2O (2 mL). The precipitated solid was separated by filtration, washed with H_2O (4×2 mL) and dried in vacuum to give 45 mg (55.1%) of **8a** as an orange solid. ^{1}H NMR ([D$_3$]acetonitrile, 500 MHz): $\delta = 0.88$ (t, 12H; CH_3), 1.21–1.40 (m, 24H; γ-, δ-, ε-CH_2), 1.59 (mc, 8H; β-CH_2), 3.45 (t, 8H; α-CH_2), 4.45 (s, 8H; benzyl-CH_2), 7.21 (s, 2H; phenyl-H), 7.29 (s, 2H; phenyl-H), 7.41–7.49 (m, 10H; py-H, phenyl-H), 7.53–7.58 (m, 8H; phenyl-H), 7.74 (s, 4H; phenyl-H),), 7.79–7.86 (m, 10H; py-H, phenyl-H), 7.92 (d, $^3J = 6$ Hz, 4H; py-H), 8.02–8.12 (m, 8H; py-H, phenyl-H), 8.39 (d, $^3J = 8$ Hz, 4H; py-H), 8.48–8.54 (m, 8H; py-H), 8.62 (m, 4H; py-H); ^{13}C NMR ([D$_3$]acetonitrile, 126 MHz): $\delta = 14.4$, 23.4, 26.6, 30.2, 32.4, 71.4, 72.2, 90.1, 124.2, 124.8, 125.3, 125.4, 125.4, 126.8, 126.8, 128.6, 128.6, 130.4, 130.9, 131.7, 132.4, 136.1, 136.4, 136.9, 138.8, 139.8, 139.8, 142.2, 149.9, 153.1, 153.1 156.7 157.9, 158.2; MS (FAB): *m*/*z* (%): 2580 (64.8), $[M - PF_6]^+$.

Deprotection of 8c: A solution of HCl in methanol (2% v/v, cat. amount) was added to a stirred solution of **8c** (90 mg, 0.03 mmol) in acetonitrile. After 3 h the solvent was removed, and the residue was dissolved in acetonitrile (4 mL). This solution added to methanol/H_2O (50/50, 4 mL). The precipitated solid was recovered by filtration, washed with H_2O ($2 \times$ 2 mL), and dried to give 64 mg (80%) of the deprotected material as an orange solid. ^{1}H NMR ($CDCl_3$, 270 MHz): $\delta = 0.90$ (t, 6H; CH_3), 1.32 (mc, 8H; hexyl-CH_2), 1.40 (mc, 4H; hexyl-CH_2), 1.61 (mc, 4H; β-CH_2), 3.42 (br s, 4H, OH), 3.49 (t, 4H; α-CH_2), 4.51 (s, 4H; benzyl-CH_2), 4.59 (8H; benzyl-CH_2), 7.25 (4H), 7.43 (4H), 7.48 (4H), 7.52 (4H), 7.55 (4H), 7.65 (2H), 7.72 (4H), 7.80 (4H), 7.85 (4H), 7.92 (4H), 8.03 (4H), 8.11 (4H), 8.39

Table 3. Crystal data and structure refinement for **1a**, **1c**, and *rac*-**7**.

	1a	**1c**	**7**
formula	$C_{110}H_{110}N_4O_4$	$C_{106}H_{111}Cl_{12}N_4O_{12}$	$C_{50}H_{48}Br_2F_{12}N_6O_5P_2Ru$
M_r	1552.02	2059.40	1363.77
T [K]	163(2)	153(2)	133(2)
λ [Å]	0.71073	0.71073	0.71073
crystal system	triclinic	triclinic	monoclinic
space group	$P\bar{1}$	$P\bar{1}$	$P2_1/c$
a [Å]	7.4113(8)	10.742(3)	18.848(3)
b [Å]	10.7138(12)	13.477(4)	13.265(2)
c [Å]	28.294(3)	17.818(6)	20.779(3)
α [°]	94.287(3)	104.796(7)	90
β [°]	97.398(3)	95.551(7)	92.556(11)
γ [°]	92.852(5)	98.434(8)	90
V [Å^3]	2217.7(4)	2442.5(14)	5190.0(14)
Z	1	1	4
ρ [Mg m^{-3}]	1.162	1.400	1.745
μ [mm^{-1}]	0.070	0.405	2.001
$F(000)$	830	1076	2728
crystal size [mm^3]	$0.34 \times 0.29 \times 0.11$	$0.60 \times 0.15 \times 0.05$	$0.58 \times 0.47 \times 0.05$
θ range [°]	1.46 – 25.03	1.94 – 22.39	1.82 – 31.51
index ranges	$-8 \le h \le 8$	$-11 \le h \le 11$	$-26 \le h \le 26$
	$-12 \le k \le 12$,	$-14 \le k \le 14$	$-18 \le k \le 19$
	$-32 \le l \le 33$	$-18 \le l \le 18$	$-30 \le l \le 29$
reflections collected	18960	14796	61133
independent reflections	7734 ($R_{int} = 0.0392$)	6035 ($R_{int} = 0.1491$)	15979 ($R_{int} = 0.0424$)
completeness to θ_{max} [%]	98.8	95.6	92.4
absorption correction	empirical	none	empirical
max./min. transmission	0.967031/0.816279	–	0.8623/0.6195
data/restraints/parameters	7734/0/532	6035/0/264	15979/0/688
goodness-of-fit on F^2	1.065	1.391	1.068
final R indices	$R_1 = 0.0703$	$R_1 = 0.2037$	$R_1 = 0.0505$
$[I > 2\sigma(I)]$	$wR_2 = 0.2027$	$wR_2 = 0.4869$	$wR_2 = 0.1499$
R indices	$R_1 = 0.1207$	$R_1 = 0.2946$	$R_1 = 0.0744$
(all data)	$wR_2 = 0.2338$	$wR_2 = 0.5332$	$wR_2 = 0.1611$
largest diff. peak/hole [e Å^{-3}]	0.709/ – 0.591	1.294/ – 0.684	2.263/ – 2.288

(4H), 8.51 (4H), 8.53 (4H), 8.54 (4H), 8.60 (4H); MS (FAB): m/z (%) = 2471 (41.6), $[M - PF_6]^+$.

X-ray structure analysis: Suitable crystals of **1a** and **1c** were obtained by slow diffusion of ethanol into a solution of **1a** in benzene or **1c** in chloroform. Crystals of *rac*-**7** were obtained by slow evaporation of the solvent from a DMSO solution over a period of several months. As the crystals of **1a**, **1c**, and *rac*-**7** all crystallize with different solvent molecules and, therefore, tend to disintegrate with loss of the included solvent molecules, the crystals were mounted out of saturated solutions at low temperature onto the tip of a glass fiber, and the data collection was performed at low temperatures with a BRUKER-AXS SMART CCD diffractometer. A total of 600 frames ($\Delta\omega = 0.3°$) for each run were collected for three ϕ positions (0°, 90°, and 240°) resulting in 1800 frames for each data set. The data were reduced to F_o^2 and corrected for absorption effects with SAINT[31] and SADABS,[32] respectively. The structures were solved by direct methods and refined by a full-matrix least-squares method (SHELXL 97[33]). The quality of the structure determination of **1c** was strongly influenced by the fact that **1c** consists of several different stereoisomers that only differ in the THP moieties and in the chloroform solvate molecules. Only one chloroform could be located in the difference Fourier map, whereas the second chloroform molecule was taken into account by means of the squeeze option in the program package PLATON.[26] As a result, the crystal only poorly diffracted at 2θ angles above 35°. Thus, only the chlorine atoms of the chloroform molecule could be refined anisotropically. After refining *rac*-**7**, three peaks in the difference Fourier map indicated the presence of a solvent molecule (most likely ethanol) in the lattice. The atomic coordinates of this solvent molecule were refined with isotropic thermal parameters for C and O. No hydrogen positions were refined for the solvent molecule. Details of the data collection and structure refinement are given in Table 3. ORTEP[34] for Windows, XSHELL,[35] and SCHAKAL97[36] were used to prepare the graphical representations. Crystallographic data (excluding structure factors) reported in this paper have been deposited with Cambridge Crystallographic Data Centre as supplementary publication nos. CCDC-167329 (**1a**), CCDC-167330 (**1b**), and CCDC-167331 (**7**). Copies of the data can be obtained free of charge on application to CCDC, 12 Union Road, Cambridge CB2 1EZ (fax: (+44) 1223-336-033; e-mail: deposit@ccdc.cam.ac.uk).

Acknowledgement

Financial support by the Deutsche Forschungsgemeinschaft (Sfb 448, TPA1) and the Fonds der Chemischen Industrie is gratefully acknowledged.

[1] a) O. Henze, D. Lentz, A. D. Schlüter, *Chem. Eur. J.* **2000**, *6*, 2362 – 2367; b) For recent related work, see: P. N. W. Baxter, *J. Org. Chem.* **2001**, *66*, 4170 – 4179.
[2] For a recent review on shape-persistant macrocycles, see: S. Höger, *J. Polym. Sci. Polym. Chem.* **1999**, 37, 2685 – 2698.
[3] For a mention of *endo*-cyclic metal complexation in a shape-persistent, all-hydrocarbon cycles, see: L. T. Scott, G. J. DeCicco, G. Reinhardt, *J. Am. Chem. Soc.* **1985**, *107*, 6546 – 6552.
[4] S. Höger, A.-D. Meckenstock, S. Müller, *Chem. Eur. J.* **1998**, *4*, 2423 – 2433.
[5] J. Zhang, J. S. Moore, *J. Am. Chem. Soc.* **1994**, *116*, 2655 – 2656.
[6] D. Venkataraman, S. Lee, J. Zhang, J. S. Moore, *Nature* **1994**, *371*, 591 – 594.
[7] G. Gattuso, S. Menzer, S. A. Nepogodiev, J. F. Stoddart, D. J. Williams, *Angew. Chem.* **1997**, 109, 1615 – 1617; *Angew. Chem. Int. Ed. Engl.* **1997**, *36*, 1451 – 1453.

[8] O. Y. Mindyuk, M. R. Stelzer, P. A. Heiney, J. C. Nelson, J. S. Moore, *Adv. Mater.* **1998**, *10*, 1363–1366.
[9] R. A. Pascal, Jr., L. Barnett, X. Qiao, D. M. Ho, *J. Org. Chem.* **2000**, *65*, 7711–7717.
[10] P. Müller, I. Usón, V. Hensel, A. D. Schlüter, G. M. Sheldrick, *Helv. Chim. Acta* **2001**, *84*, 778–785.
[11] G. D. Hartgerink, T. D. Clark, M. R. Ghadiri, *Chem. Eur. J.* **1998**, *4*, 1367–1372.
[12] For shape-persistent macrocycles with liquid crystalline properties see, for example: S. Höger, V. Enkelmann, C. Tschierske, *Angew. Chem.* **2000**, *112*, 2356–2358; *Angew. Chem. Int. Ed.* **2000**, *39*, 2268–2270.
[13] D. H. Cobden, *Nature* **2001**, *409*, 32–33.
[14] T. W. Greene, P. G. M. Wuts, *Protective Groups in Organic Synthesis*, Wiley, New York, **1991**.
[15] O. Henze, U. Lehmann, A. D. Schlüter, *Synthesis* **1999**, 683–687.
[16] V. Hensel, A. D. Schlüter, *Chem. Eur. J.* **1999**, *5*, 421–429.
[17] Y. Yamamoto, A. Yanagi, *Chem. Pharm. Bull.* **1982**, *30*, 1731–1737.
[18] J. Tsuji, *Palladium Reagents and Catalysts*, Wiley, Chichester, **1995**.
[19] U. Lehmann, A. D. Schlüter, *Eur. J. Org. Chem.* **2000**, 3483–3487.
[20] V. Hensel, K. Lützow, J. Jakob, K. Geßler, W. Saenger, A. D. Schlüter, *Angew. Chem.* **1997**, *109*, 2768; *Angew. Chem. Int. Ed. Engl.* **1997**, *36*, 2654.
[21] For an example with lower yield, see: M. Schmittel, H. Ammon, *Synlett* **1999**, 750–752.
[22] J. S. Moore, J. Zhang, *Angew. Chem.* **1992**, *104*, 873–874; *Angew. Chem. Int. Ed. Engl.* **1992**, *31*, 922–924; S. Höger, A.-D. Meckenstock, H. Pellen, *J. Org. Chem.* **1997**, *62*, 4556–4557.
[23] A. Juris, V. Balzani, F. Barigelletti, S. Campagna, P. Belser, A. V. Zelewsky, *Coord. Chem. Rev.* **1988**, *84*, 85–277.
[24] V. Balzani, A. Juris, M. Venturi, S. Campagna, S. Serroni, *Chem. Rev.* **1996**, *96*, 759–833.
[25] X. Hua, A. V. Zelewsky, *Inorg. Chem.* **1995**, 5791–5797.
[26] PLATON/PLUTON: a) A. L. Spek, *Acta Crystallogr. Sect A* **1990**, *46*, C34–C40; b) A. L. Spek, PLATON, A Multipurpose Crystallographic Tool, Utrecht University, Utrecht (The Netherlands), **1998**.
[27] a) G. A. Jeffrey, L. Lewis, *Carbohydr. Res.* **1978**, *60*, 179–184; b) R. Taylor, O. Kennard, *Acta Crystallogr. Sect. B* **1983**, *39*, 133–136.
[28] WINGX: a) L. J. Farrugia, *J. Appl. Crystallogr.* **1999**, *32*, 837–838; PARST: b) M. Nardelli, *Comput. Chem.* **1983**, *7*, 95–97; c) M. Nardelli, *J. Appl. Crystallogr.* **1995**, *28*, 659.
[29] We would like to thank one of the referees for pointing out that the use of the word "channel" may lead to the perception that the crystals, especially that of **1c**, actually contain some empty geometrically confined compartments amenable to transportation. The "channels" are certainly filled with solvent molecules and parts of the solubilizing chains, whereby the latter could be described as "hairs" dangling into the "channel's" interior and leaving enough space for motion of the solvent molecules. In this sense the word channel does seem acceptable to us.
[30] Complex **8c**: ^{1}H NMR ($CDCl_3$, 270 MHz): $\delta = 0.85$ (mc, 6H; CH_3), 1.21 (mc, 8H; hexyl-CH_2), 1.36 (mc, 4H; hexyl-CH_2), 1.58 (mc, 20H; THP, β-CH_2), 1.72 (mc, 4H; THP), 1.79 (mc, 4H; THP), 3.43–3.58 (mc, 4H; α-CH_2, THP), 3.82 (mc, 4H; THP), 4.41 (d, 4H; benzyl-CH_2), 4.50 (s, 4H; THP), 4.68 (s, 8H; benzyl-CH_2), 7.24 (s, 4H), 7.44 (mc, 8H), 7.51 (s, 4H), 7.58 (s, 4H), 7.72 (s, 4H), 7.78–7.84 (m, 10H), 7.89 (d, 4H), 8.02–8.10 (m, 8H), 8.47–8.55 (m, 8H), 8.61 (d, 4H); MS (FAB): *m*/*z* (%): 2808 (95) $[M - PF_6]^+$. Deprotected **8c**: ^{1}H NMR ($CDCl_3$, 270 MHz): $\delta = 0.90$ (t, 6H; CH_3), 1.32 (mc, 8H; hexyl-CH_2), 1.40 (mc, 4H; hexyl-CH_2), 1.61 (mc, 4H; β-CH2), 3.42 (br s, 4H; OH), 3.49 (t, 4H; α-CH_2), 4.51 (s, 4H; benzyl-CH_2), 4.59 (s, 8H; benzyl-CH_2), 7.25, 7.43, 7.48, 7.52, 7.55, 7.65, 7.72, 7.80, 7.85, 7.92, 8.03, 8.11, 8.39, 8.51, 8.53, 8.54, 8.60 (17 × s, 4H); MS (FAB): *m*/*z* (%): 2471 (42) $[M - PF_6]^+$.
[31] SAINTPLUS: Software Reference Manual, Version 5.054, Bruker-AXS, Madison, WI, **1997–1998**.
[32] R. H. Blessing, *Acta Crystallogr. Sect A* **1995**, *51*, 33–38; SADABS: Bruker AXS **1998**.
[33] G. M. Sheldrick, SHELX97 Programs for Crystal Structure Analysis (Release 97-2), Universität Göttingen, Göttingen (Germany), **1998**.
[34] ORTEP3 for Windows: L. J. Farrugia, *J. Appl. Crystallogr.* **1997**, *30*, 565.
[35] XSHELL: Bruker-AXS, Madison, WI, **1998**.
[36] SCHAKAL: E. Keller, *J. Appl. Crystallogr.* **1989**, *22*, 12–22.

Received: July 19, 2001 [F3426]